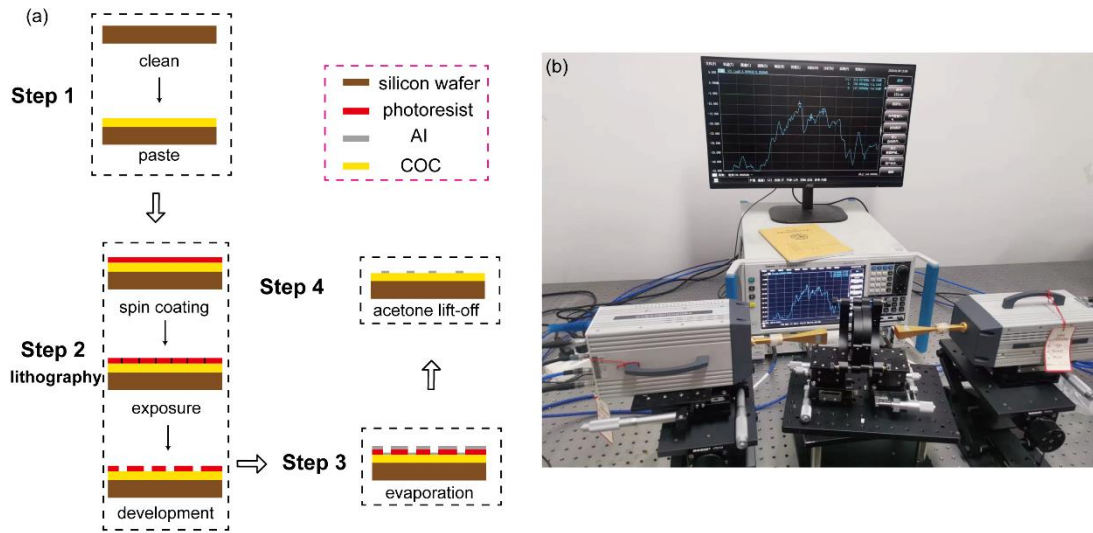


# Supplementary Document for Mechanically Reconfigurable Terahertz Polarization Converter by Coupling-Mediated Metasurfaces

## 1. Sample fabrication process and assembled measurement system

The sample fabrication process and the assembled measurement system are illustrated in Fig. S1(a) and Fig. S1(b), respectively.



**Fig. S1.** (a) Flow chart of sample fabrication based on COC thin film. (b) Photo of the assembled measurement system.

## 2. Effect of relative metasurface movement on LP converter performance

Here, we investigate the impact of the in-plane movement of one metasurface relative to the other on the performance of the LP converter when the air-gap distance between the two pieces of the sample corresponds to the optimal value ( $d = 460 \mu\text{m}$ ). The bright-mode resonator is shifted horizontally and vertically along the  $x$  and  $y$  directions by  $500 \mu\text{m}$ , while the dark-mode resonator is fixed. The amplitude transmissions for co- and cross-polarization are observed through simulation and

experiment, and the PCR is calculated.

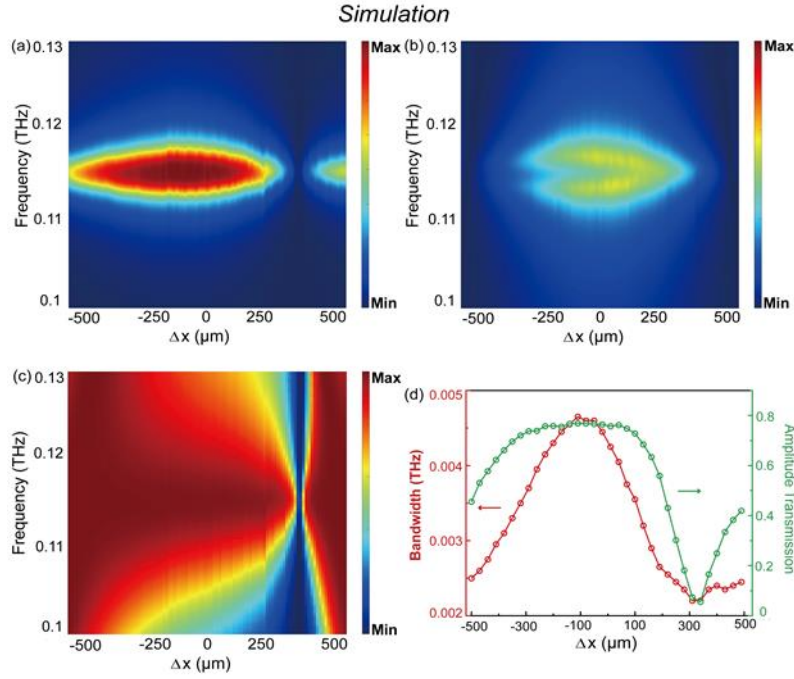


**Fig. S2.** Simulation results for relative  $x$ -axis shift of one metasurface at the optimal air-gap. (a) Cross-polarization amplitude transmission, (b) co-polarization amplitude transmission, and (c) PCR spectrum as a function of  $d$  from 150 to 800  $\mu\text{m}$  under normal incidence within the frequency range from 0.1 to 0.13 THz. (d) Bandwidth and amplitude transmission of the cross-polarization component at the center frequency of 0.115 THz as a function of  $d$  from 150 to 800  $\mu\text{m}$ .

The simulated cross- and co-polarization transmission spectra for movement along the  $x$  direction are shown in Fig. S2(a) and Fig. S2(b), respectively. A significant high-transmission region is observed within the frequency range from 0.11 to 0.12 THz, with the maximum occurring near  $\Delta x = 0$   $\mu\text{m}$ . This indicates that the energy of the bright mode is most efficiently transferred to the dark mode when the two metasurfaces are centered, thus minimizing energy loss. Relative in-plane movement of one resonator affects the PCR of the device negatively, as shown in Fig. S2(c), preventing effective energy propagation between the resonators. This increased energy loss disrupts the resonance conditions, thereby reducing the coupling efficiency. The simulation results for the bandwidth and the amplitude at the center frequency of cross-polarization

transmission are shown in Fig. S2(d). These results demonstrate that the in-plane lateral movement of one metasurface significantly affects the polarization conversion performance, with the optimal state obtained for centered alignment.

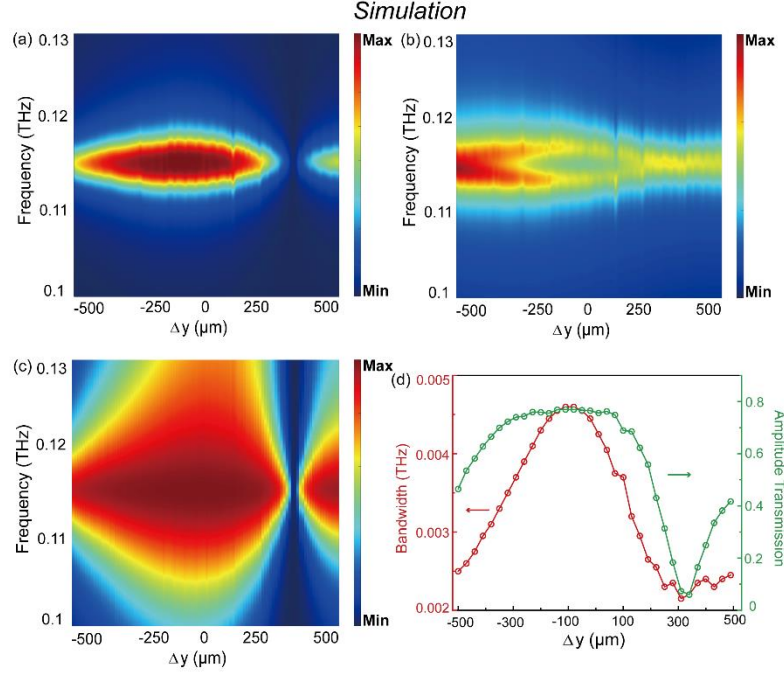


**Fig. S3.** Simulation results for relative  $y$ -axis shift of one metasurface at the optimal air-gap. (a) Cross-polarization amplitude transmission, (b) co-polarization amplitude transmission, and (c) PCR spectrum as a function of  $d$  from 150 to 800  $\mu\text{m}$  under normal incidence within the frequency range from 0.1 to 0.13 THz. (d) Bandwidth and amplitude transmission of the cross-polarization component at the center frequency of 0.115 THz as a function of  $d$  from 150 to 800  $\mu\text{m}$ .

Similarly, the simulation results for moving one metasurface along the  $y$  direction are shown in Fig. S3(a) through Fig. S3(d) and are comparable to the results obtained for movement along the  $x$  direction. Figure S4(a) through Fig. S4(d) represent the experimental results for movements along the  $x$  and  $y$  directions. At the beginning of measurement, the two metasurfaces need to be in close contact, ensuring that the alignment marks of both are perfectly overlapped. After that, the longitudinal knobs of the 2D displacement stages are rotated to separate the two parts to the optimal gap. Then, by adjusting the transverse knobs of the 2D displacement stages and the control

knobs of the lift stages, the resonators are precisely moved to the specified distances along the  $x$  and  $y$  directions. The experimental results generally show consistency with the simulations, verifying the accuracy of the model design and the validity of the experimental system.

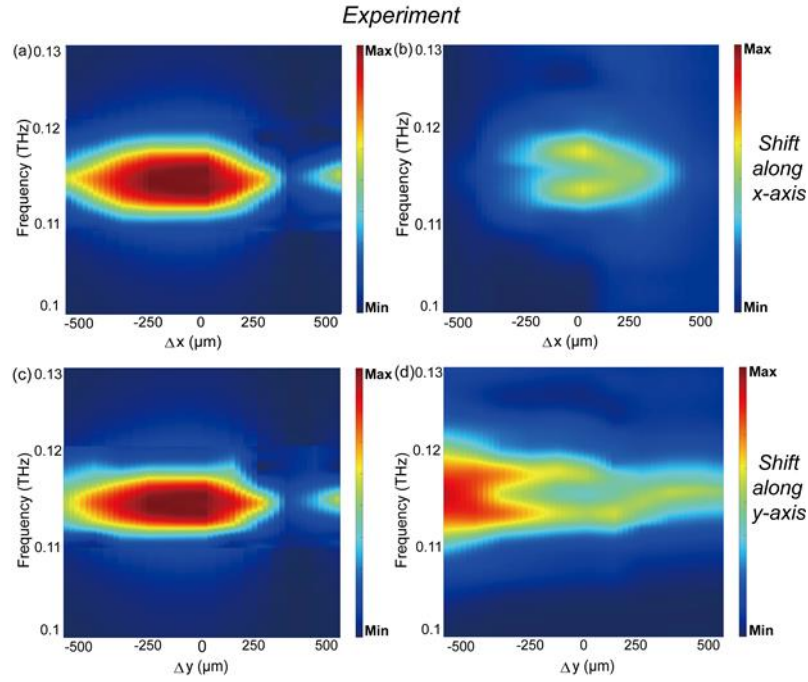


**Fig. S4.** Measurement results for relative  $x$ - and  $y$ -axis shifts of one metasurface at the optimal air gap. (a) and (b) Cross- and co-polarization amplitude transmissions for  $x$ -axis shift, respectively. (c) and (d) Cross- and co-polarization amplitude transmissions for  $y$ -axis shift, respectively.